



Contents lists available at ScienceDirect

Nuclear Instruments and Methods in Physics Research A

journal homepage: www.elsevier.com/locate/nima

Thermoluminescence kinetic analysis of quartz using an improved general order model for exponential distribution of activation energies

M. Zahedifar*, S. Harooni, E. Sadeghi

TL Laboratory, Physics Department, University of Kashan, Kashan, Islamic Republic of Iran

ARTICLE INFO

Article history:

Received 21 December 2010

Received in revised form

6 June 2011

Accepted 28 June 2011

Available online 5 July 2011

Keywords:

Thermoluminescence

General order

Continuous trap

Exponential distribution

Quartz

ABSTRACT

A modified thermoluminescence general order model has been presented for an exponential distribution of trapping states, which fairly approaches the corresponding first and second orders of kinetics. The proposed model was used for kinetic analysis of thermoluminescence glow curve of quartz from the central zone of Iran. Results show that the presented model is thoroughly applicable in real thermoluminescence glow peaks.

© 2011 Elsevier B.V. All rights reserved.

1. Introduction

Quartz is the second most abundant mineral (after feldspar) in the continental crust of the earth. It is a common mineral in many igneous, metamorphic and sedimentary rocks. The trace element compositions and the defect structure are determined mostly by the conditions at the time of formation, which vary in different crystallization environments [1]. Due to good luminescence properties of quartz, it is usually employed in retrospective dosimetry and dating [2–5]. The use of thermoluminescence (TL) as a dating tool has frequently relied on quartz as the principal dosimeter material, however each quartz mineral extracted from different regions of the world may exhibit different TL properties [6]. Because of routine application of quartz for estimating archeological dose, determination of its trapping parameters is important since analysis of lifetime of TL peaks and therefore the time range over which it might be useful for dating need precise information about its kinetic parameters. The estimation of kinetic parameters of stable TL peaks of natural quartz is an active area of research and various techniques have been devoted to deduce the parameters from the glow curves. Most of the methods applied for determination of kinetic parameters rely on trapping states with a sharp activation energy and there are widely different values of trap parameters reported in the literature because of differences in the origin of the quartz, impurity content and the methods used to derive the

trapping parameters [7–10]. Hornyak et al. found it necessary to attribute a distribution of activation energies to the 375 °C glow peak of quartz sample from the Kalahari desert to allow for a significant retrapping [11]. Assuming a Gaussian distribution of activation energies, they obtained a value of 1.45 eV for the center of the distribution. Considering the anomalous behavior of the high temperature (at about 320 °C) TL glow peak of a Nigerian quartz, it has been explained on the assumption that the peak may be complex consisting of several overlapping glow peaks [12]. The quartz sample extracted from the central zone of Iran, has a main TL glow peak with descending part extended over a large temperature region. None of the glow peaks produced by the use of existing TL models with sharp activation energy can be fitted to the glow peaks of quartz sample from Iran. In this work first a model is developed for determination of trapping parameters of a TL glow peak having a continuous and exponential distribution of activation energies and then it is applied to the quartz sample from Iran. It is shown that the experimental glow peaks are fairly fitted to the glow peaks produced by the proposed model. The applicability of this model to other important materials is also discussed.

2. Function for general order of kinetics

May and Partridge [13] presented a general order kinetic model for TL glow peaks as following:

$$I(T) = -\beta \frac{dn}{dT} = \frac{s}{n_0^{b-1}} n^b \exp\left(-\frac{E}{kT}\right) \quad (1)$$

* Corresponding author. Tel.: +98 5912577; fax: +98 5514005.
E-mail address: zhdfr@kashanu.ac.ir (M. Zahedifar).

where $T(K)$ is the temperature, β ($K s^{-1}$) is the linear heating rate, n (cm^{-3}) the concentration of trapped electrons, s (s^{-1}) the frequency factor, n_0 (cm^{-3}) the initial concentration of trapped electrons, E (eV) the activation energy and k (eVK^{-1}) the Boltzman's constant. In this model b is the order of kinetics, which varies between 1 (dominant recombination) and 2 (dominant retrapping) and somewhat beyond this range. Therefore Eq. (1) is capable of better conforming to the experimental glow peaks than the first and second orders of kinetic.

Rasheedy [14] believed that previous workers have suggested an equation for the general order kinetics of a TL glow peak, which cannot be explained by the usual first or second order of kinetics. He presented the equation of the general order model as follows:

$$I(T) = -\beta \frac{dn}{dT} = \frac{s}{N^{b-1}} n^b \exp\left(-\frac{E}{kT}\right) \quad (2)$$

where N (cm^{-3}) is the concentration of trapping states. This equation is superior than that presented by May and Partridge since Eq. (2) reduces to the first and second order of kinetics for $b=1$ and $b=2$ while Eq. (1) does not meet the second order of kinetics on inserting $b=2$ in the function describing the TL intensity [14]. The kinetic order b can be related to the shape of the glow peak via the asymmetry factor defined as $(T_2 - T_m)/(T_2 - T_1)$ in which $T_2 - T_1$ is the full width at half maximum (FWHM) and T_m is the temperature of maximum intensity. On increasing the kinetic order from 1 to 2, the asymmetry factor increases from 0.42 to 0.52. But in some cases we encounter glow peaks with the descending part extended over a wide temperature range having the asymmetry factor far beyond the limiting value of 0.52. Feldspar [15], basaltic rocks [16] and quartz from the central zone of Iran are as such samples. In the following section we attempt to generalize Eq. (2) to a TL model with an exponential distribution of activation energies. It will be shown that the glow peaks produced from the resulting equation fairly fit to the experimental TL glow peaks with extended high temperature tail.

3. Proposed theoretical equation

Solving Eq. (2) for n results

$$n = n_0 \left(1 + \left(\frac{n_0}{N}\right)^{b-1} \frac{s}{\beta} (b-1) \int_{T_0}^T \exp\left(-\frac{E}{kT'}\right) dT' \right)^{-\frac{1}{b-1}} \quad (3)$$

For a continuous and uniform distribution of trapping centers over an energy range of $\Delta E = E_2 - E_1$, the equation for $n(E)$ yields

$$n(E) dE = \frac{n_0}{\Delta E} \left(1 + \left(\frac{n_0}{N}\right)^{b-1} \frac{s}{\beta} (b-1) \int_{T_0}^T \exp\left(-\frac{E}{kT'}\right) dT' \right)^{-\frac{1}{b-1}} dE \quad (4)$$

Then

$$n = \int_{E_1}^{E_2} \frac{n_0}{\Delta E} \left(1 + \left(\frac{n_0}{N}\right)^{b-1} \frac{s}{\beta} (b-1) \int_{T_0}^T \exp\left(-\frac{E}{kT'}\right) dT' \right)^{-\frac{1}{b-1}} dE \quad (5)$$

For a continuous and uniform distribution of trapping centers, Eqs 2 and 5 result in

$$I(T) = \left(\frac{n_0}{N}\right)^{b-1} s \int_{E_1}^{E_2} \frac{n_0}{\Delta E} \exp\left(-\frac{E}{kT}\right) \times \left(1 + \left(\frac{n_0}{N}\right)^{b-1} \frac{s}{\beta} (b-1) \int_{T_0}^T \exp\left(-\frac{E}{kT'}\right) dT' \right)^{-\frac{b}{b-1}} dE \quad (6)$$

Eq. (6) can be transformed in order to describe a general order glow peak with an exponential distribution of activation energies by replacing $n_0/\Delta E$ (density of states for a uniform distribution of activation energies) with

$$n(E) = n_0 \exp\left(-\frac{E-E_0}{\sigma}\right) / \sigma$$

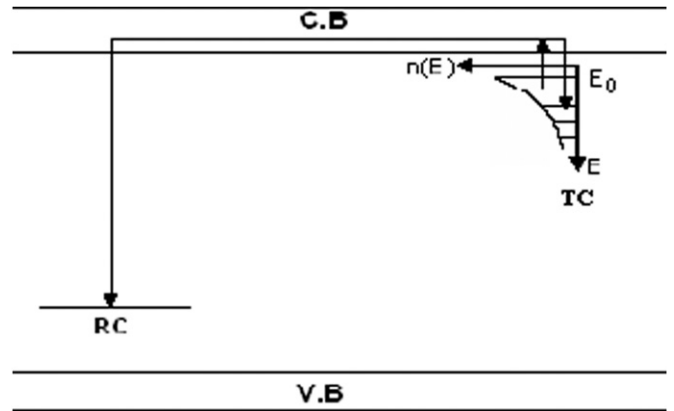


Fig. 1. Schematic energy level diagram for one recombination center and a continuously distributed trapping states with exponential shape.

which gives the density of states for a continuous and exponential distribution of trapping states.

$$I(T) = \left(\frac{n_0}{N}\right)^{b-1} s \int_{E_0}^{\infty} \frac{n_0}{\sigma} \exp\left(-\frac{E-E_0}{\sigma}\right) \exp\left(-\frac{E}{kT}\right) \times \left(1 + \left(\frac{n_0}{N}\right)^{b-1} \frac{s}{\beta} (b-1) \int_{T_0}^T \exp\left(-\frac{E}{kT'}\right) dT' \right)^{-\frac{b}{b-1}} dE \quad (7)$$

Eq. (7) is the desired general order thermoluminescence glow curve deconvolution (GCD) function, which describes a TL glow peak with an exponential distribution of trapping states and effective kinetic order of b . Fig. 1 shows the level scheme for an exponential distribution of trapping states along with the possible transitions between trapping center (TC), conduction band and the recombination center (RC). In Fig. 1, E_0 is the shallower trapping state, which is measured relative to the edge of the conduction band and the parameter σ determines the width of the energy distribution (an energy interval from E_0 to a specific energy corresponding to $n(E)/e$).

It is worth noting that for a continuous distribution of trapping states the kinetic order b does not bear the same meaning as in the general order model with a sharp activation energy. In a continuous distribution of trapping states, once the retrapping is allowed, the charge carriers can be retrapped at any energy level in the continuous distribution of trapping states, but not necessarily at the same energy level from which they are thermally excited; thus we refer it as an effective kinetic order. Heating of the sample was done at a constant rate.

As pointed out, the presented function for TL intensity reduces to the first order model by closing b to 1 and entirely coincides to the second order of kinetics by simply equating $b=2$ in Eq. (7). Also as will be illustrated, the relationship between the effective kinetic order and the symmetry of the glow peak is altered in the case of continuous activation energies.

4. Synthetic glow peaks and comparisons

The function describing the TL intensity for the first order of kinetic with exponential distribution of trapping states is [16]

$$I(T) = \frac{n_0 s}{\sigma} \int_{E_0}^{\infty} \exp\left(-\frac{E-E_0}{\sigma}\right) \times \exp(-E/kT) \exp\left[-\frac{s}{\beta} \int_{T_0}^T \exp(-E/kT') dT'\right] dE \quad (8)$$

It is a simple task to show that the glow curves produced using Eq. (7) will entirely coincide with those created using Eq. (8). It is sufficient to fit the synthetic TL glow curve of the proposed general order model to the corresponding first order model by setting $b \approx 1$ in it. A program produced in our laboratory using the Levenberg–Marquart algorithm based on non-linear least square method was employed for glow curve deconvolution (GCD) and for obtaining the trapping parameters of glow peaks. For testing the goodness of fit, the figure of merit (FOM) was used [17]

$$\text{FOM} = \sum_{j_f}^{j_i} \frac{100|y_i - y(x_i)|}{A} \quad (9)$$

in which j_f and j_i are the numbers of the first and the last channel (temperature interval, ΔT) used for curve fitting, y_i is the intensity obtained from the first order model (Eq. (8)), $y(x_i)$, the intensity expected from Eq. (7) and A , the total area of fitted glow peak between j_f and j_i . Fig. 2 (open circles) shows the synthetic glow peaks produced using first order model for exponential distribution of activation energies (Eq. (8)). Solid lines show the fitted general order peaks given by Eq. (7) with $b=1.001$. FOM values are lower than 0.05, which show that the glow curves produced using the proposed function for general order of kinetics (Eq. (7)) in the limiting case of $b \approx 1$ are the same as the glow curves depicted by the first order model (Eq. (8)). Three-dimensional glow peaks produced for different values of $b=0.01$, 1.5, 1.9 are shown in Fig. 3(a)–(c). As is evident, for a given value of the kinetic order b , an increase in the parameter σ (the width of the energy distribution), causes the high temperature end of the glow peak to shift to higher temperatures. Increasing the kinetic order has the same effect on the symmetry of the glow peak as the parameter σ . Variation of the asymmetry factor with parameter σ for different values of b is shown in Fig. 4. It is evident that for lower values of σ the relation between b and the asymmetry factor is approximately the same as is expected for a glow peak with sharp activation energy. However increasing the width of the energy distribution, causes the asymmetry factor to shift to higher values for each specified value of the parameter b . For higher values of σ , this parameter has a paramount role on the symmetry of the glow peaks therefore the asymmetry factors obtained from the proposed model for different values of b come close to each other for higher values of σ .

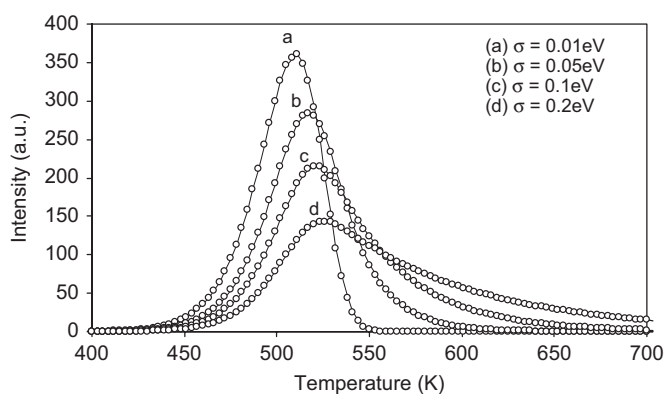


Fig. 2. Fitting of the proposed general order model with exponential distribution of activation energies and kinetic parameters $b=1.001$, $N=1 \times 10^9 \text{ (cm}^{-3}\text{)}$, $n_0=8 \times 10^3 \text{ (cm}^{-3}\text{)}$, $s=1 \times 10^{12} \text{ (s}^{-1}\text{)}$, $E_0=1.3 \text{ eV}$, $\beta=2 \text{ (K s}^{-1}\text{)}$ and (a) $\sigma=0.01 \text{ eV}$, (b) $\sigma=0.05 \text{ eV}$, (c) $\sigma=0.1 \text{ eV}$ and (d) $\sigma=0.2 \text{ eV}$ (solid lines) to the first order model (open circles). As is observed in this limiting case, our proposed model gives entirely the same results compared to the first order model.

5. Experimental procedure

Quartz sample were produced from Yazd, located at the central zone of Iran. The whole procedure of sample preparation was performed under dark room condition. First, the surface layer of the sample, which had been exposed to light, was removed. For obtaining a uniform powder, the quartz rocks were milled and sieved to mesh size 80–100 μm . Then the produced yellow colored sample was washed in 10% hydrochloric acid to dissolve the carbonate. The structural characterization of the sample was supported by X-ray diffraction (XRD) with Rigaku D-maxcIII diffractometer using $\text{CuK}\alpha$ radiation. X-ray fluorescence (XRF) spectrometer was used for the mineralogical analysis and identifying the type and concentration of different impurities contained in the natural quartz. All TL readouts were taken in a Harshaw model 4500 computer based TL reader using a contact heating where the temperature of the heater strip (planchet) is recorded as indicator of the temperature of the sample with a precision of 1 $^\circ\text{C}$. For reducing the thermal lag inside the powder sample, the sample powder was placed as a thin layer on the planchet and a low heating rate of 2 $^\circ\text{C/s}$ was used for recording the glow curves with preheating of 50 $^\circ\text{C}$ to a maximum temperature of 500 $^\circ\text{C}$ in nitrogen atmosphere. Kinetic parameters assigned to the TL peaks are averages of seven readouts of the samples of same mass.

6. Experimental results

Fig. 5 shows the X-ray diffraction profile (powder method) of the quartz sample from Iran. All diffraction peaks match well with the characteristic peaks of SiO_2 and XRF analysis gives its concentration to be 98.68%. The Type and concentration of different impurities are also observed in Table 1 as a result of XRF analysis of the quartz sample. Kinetic analysis of TL glow peaks of quartz has been performed using the proposed general order model for continuous and exponential distribution of trapping centers. Because of the vital importance of natural TL (NTL) (thermally stimulated luminescence due to the total dose received by the sample from environmental radiation fields during its archeological lifetime) in archeological chronology, NTL glow curve of quartz sample was exploited for determination of the trapping parameters. All samples showed TL growth when additive doses were applied to the natural dose, indicating that their NTL was not in saturation. This is a necessary condition for the proposed model to be appropriate for TL kinetic analysis. NTL glow curve of this mineral exhibits a small peak at about 270 $^\circ\text{C}$, a main broad peak at about 360 $^\circ\text{C}$ and a high temperature peak and resemble those of volcanic quartz [18]. Fig. 6(a) shows the total glow curve of quartz sample. Thermal bleaching method was exploited in order to record the TL glow curve of high temperature peak (b). Using this method, the sample was first annealed in TLD reader at a constant heating rate up to a temperature corresponding to the end of the main peak. This procedure empties all the trapping states responsible for the main peak. In subsequent readout of the sample, merely the high temperature tail of the glow curve was recorded (Fig. 6(b)). The glow curve, including both the main peak and the low temperature peak were obtained by subtracting the ascending part of the high temperature peak from the total glow curve. Using the proposed model and the fitting program, the first and second peaks of quartz sample were deconvoluted. Estimated values for trapping parameters achieved using GCD procedure along with the accuracies in E_0 and s are given in Table 2. The width of distribution of trapping states obtained for low temperature peak (c) in Fig. 6 is negligible, which indicates that a sharp activation energy is attributed to this glow peak. As pointed out in Section 5, all the

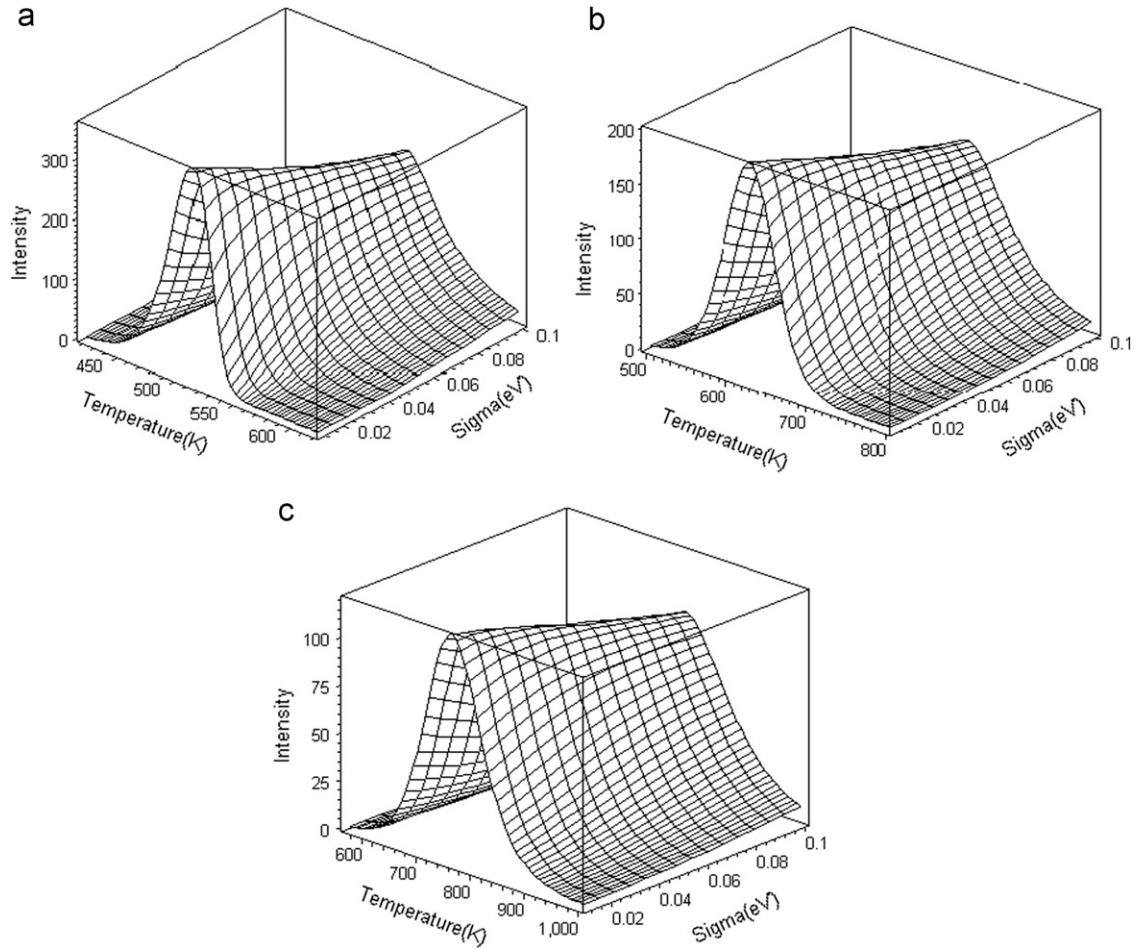


Fig. 3. Glow peaks produced using the new general order model with the same kinetic parameters as in Fig. 2 and (a) $b=1.01$, (b) $b=1.5$ and (c) $b=1.9$ and different values of σ . As is evident, an increase in b causes the descending part of the glow peaks to shift to higher temperatures.

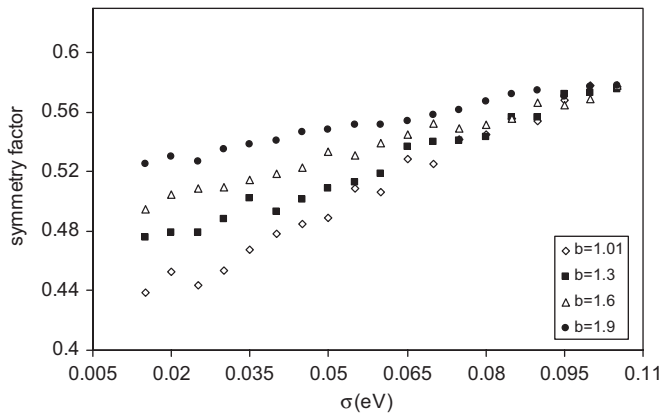


Fig. 4. Variation of asymmetry factor with the width of energy distribution σ for different values of b . As shown, when the parameter σ approaches zero (which corresponds to single activation energy) the expected relation between asymmetry factor and b appears. But for higher values of σ the asymmetry factor is approximately the same for different values of b .

experimental results are averages over seven readouts of the uniform powder sample of the same mass. Fig. 7 shows the glow curves of the quartz sample recorded after post irradiation anneal up to T_{stop} in a range between 300 and 400 °C. As is seen, on

increasing T_{stop} , the main glow peak shifts continuously towards higher temperatures. The peak area, which indicates the population of trapping states and the maximum intensity also decrease continuously, while the high temperature part of the glow peak remains unaffected. This indicates that the broad peak of this sample obeys continuous energy distribution [19]. Increasing the preheat temperature (T_{stop}) causes emptying of the shallower energy levels in the continuous energy distribution. Therefore cooling the phosphor followed by subsequent recording of the glow curve results in a shift of the initial rise region of the glow peak to higher temperatures while the high temperature tail remains unchanged. Consequently we expect the parameter E_0 (the edge of continuous energy distribution near to conduction band) to shift to higher values with increasing T_{stop} . The same procedure of obtaining the kinetics parameters as discussed for Fig. 6 were applied for the determination of kinetic parameters of the main glow peak recorded following different values of T_{stop} . All the main glow peaks obtained after pre-heating up to different T_{stop} were fitted well with the proposed general order model with exponential distribution of trapping states. Obtained results for kinetic parameters of the main peak using different T_{stop} values are presented in Table 3. On increasing T_{stop} , population of trapping states decreases and retrapping to recombination ratio increases. Therefore an increase in the effective kinetic order b with increasing T_{stop} in Table 3 can be attributed to a decrease in the population of trapping states.

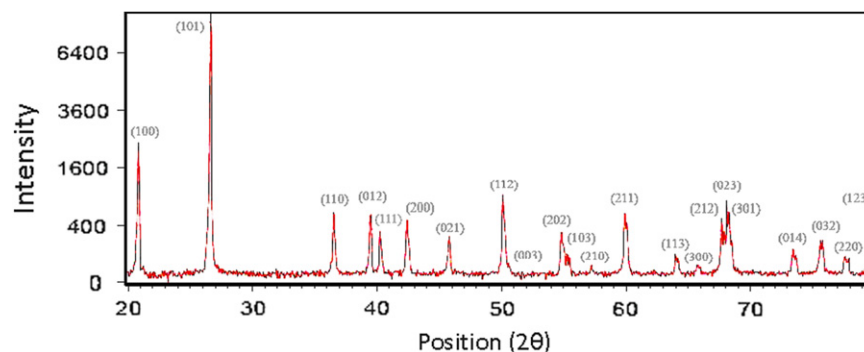


Fig. 5. X-ray diffraction pattern of the quartz sample.

Table 1

The result of XRF analysis of the quartz sample.

Compound	SiO ₂	Fe ₂ O ₃	Al ₂ O ₃	SO ₃	CaO	Cr ₂ O ₃	K ₂ O	CuO
Concentration (%)	98.68	0.494	0.430	0.140	0.065	0.047	0.022	0.011

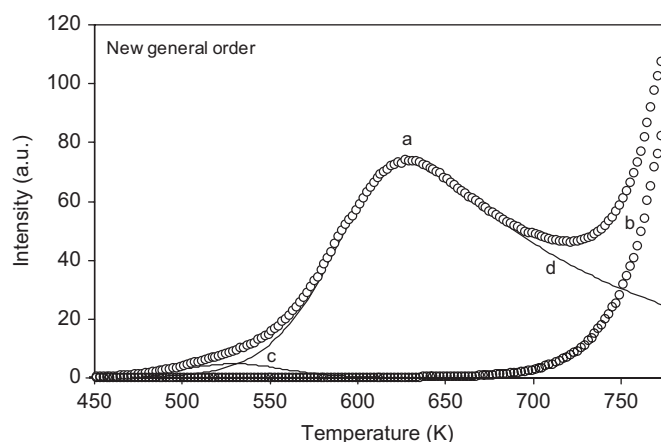


Fig. 6. Total glow curve (a) and initial rise region of high temperature peak (b), which was obtained after thermal bleaching of lower temperature peaks (open circles). By subtracting the curves (a) and (b) the main glow curve was obtained. Finally the GCD procedure was used to obtain the low temperature peak (c) and the main peak (d).

Table 2

Kinetic parameters of the first and second peaks of quartz sample.

Peak	<i>b</i>	<i>N</i>	<i>n</i> ₀	<i>s</i> (s ⁻¹)	<i>σ</i> (eV)	<i>E</i> ₀ (eV)
One	1.56	1.06e7	179	$(7.66 \pm 2.33) \times 10^{11}$	–	1.06 ± 0.05
Two	1.27	1.20e9	6740	$(2.63 \pm 2.33) \times 10^{10}$	0.25	1.19 ± 0.06

7. Discussion

An improved general order TL glow curve deconvolution function with exponential distribution of activation energies has been presented. The main advantage of the proposed function is that it fairly approaches the limiting cases of first and second orders of kinetics while the May–Partridge model as starting point for deriving a TL model for continuous distribution of trapping states encounters problems for the limiting case of $b=2$. As is evident in Figs. 6 and 7, the main glow peak of quartz sample from Iran has an elongated descending part with asymmetry factors far beyond 0.52. Therefore TL models corresponding to a specific activation energy, which predict a maximum

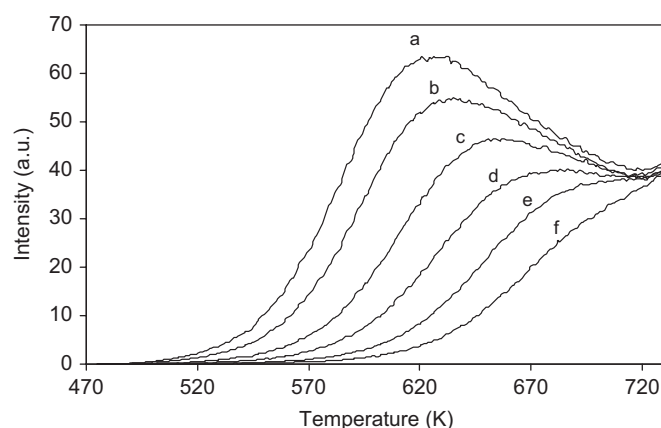


Fig. 7. The main glow peak of quartz recorded for different values of T_{stop} 300 °C (a), 320 °C (b), 340 °C (c), 360 °C (d), 380 °C (e) and 400 °C (f). As is seen, an increase in T_{stop} causes the whole glow peak to shift continuously to higher temperatures.

Table 3

Determined kinetic parameters of the main glow peak of the quartz sample for different values of T_{stop} using the proposed model for glow curve fitting.

T_{stop} (°C)	<i>b</i>	<i>N</i>	<i>n</i> ₀	<i>s</i> (s ⁻¹)	<i>σ</i> (eV)	<i>E</i> ₀ (eV)
300	1.48	1.2×10^9	6304	$(6.20 \pm 2.45) \times 10^{12}$	0.28	1.32 ± 0.04
320	1.53	1.2×10^9	5720	$(8.30 \pm 3.31) \times 10^{12}$	0.29	1.33 ± 0.07
340	1.55	1.2×10^9	4668	$(1.12 \pm 2.04) \times 10^{11}$	0.30	1.37 ± 0.03
360	1.65	1.2×10^9	4052	$(2.40 \pm 1.84) \times 10^{13}$	0.30	1.38 ± 0.06
380	1.70	1.2×10^9	3622	$(5.80 \pm 3.19) \times 10^{13}$	0.31	1.44 ± 0.06
400	1.75	1.2×10^9	3472	$(8.00 \pm 4.50) \times 10^{13}$	0.33	1.46 ± 0.02

asymmetry factor of 0.52 cannot be employed for kinetic analysis of the main glow peak (at about 360 °C) of this sample. Despite of evident differences between the shape of high temperature peak of the quartz sample from Iran and those from the other continental crust of the earth, there are reported activation energies for the glow peak around 360 °C, which lie in the range of continuous distribution of activation energies obtained in this study [6,10,11]. It is worth noting that the main TL glow peak of feldspar, which is the most abundant mineral in the crust of the earth with important application in retrospective dosimetry[20]

and volcanic quartz [18] resembles the main glow peak of quartz sample of Iran. It also Fig. 3 reveals that both the kinetic order and width of the energy distribution have the same effect in increasing the symmetry factor of glow peak. Therefore the proposed general order model gives more accurate value for the width of the energy distribution σ , compared to the analogous first order model [16], which overestimates the width of energy distribution for glow peaks with non first order behavior. Excellent fitting of the main glow peak of quartz from Iran to the glow peaks produced using the proposed model and resemblance of the main TL glow peaks of feldspar, volcanic quartz and quartz from Iran reveals that the proposed model is applicable in important real TL materials.

References

- [1] F. Preusser, M.L. Chithambo, T. Gotte, M. Martini, K. Ramseyer, E.J. Sendezeva, G.J. Susino, A.G. Wintle, *Earth-Sci. Rev.* 97 (2009) 184.
- [2] M.G. Aitken, *Thermoluminescence Dating*, Academic Press, New York, 1985.
- [3] M.S. Abdel-Wahab, S.A. El-Fiki, M.A. El-Fiki, M. Gomaa, S. Abdel-Kariem, M. El-Faramawy, *Radiat. Phys. Chem.* 47 (5) (1996) 697.
- [4] T. Watanuki, A.S. Murray, S. Tsukamoto, *Earth Planet. Sci. Lett.* 240 (2005) 774.
- [5] Santa Chalwa, T.K. Gundu Rao, A.K. Sinchvi, *Radiat. Meas.* 29 (1) (1998) 53.
- [6] J. Porkein, G.A. Wagner, *Radiat. Meas.* 23 (1) (1994) 85.
- [7] A.N. Yazici, M. Topaksu, *J. Phys. D: Appl. Phys.* 36 (2003) 620.
- [8] I. Veronese, A. Giussani, H.Y. Goksu, M. Martini, *Radiat. Meas.* 38 (2004) 743.
- [9] S.A. Petrov, I.K. Bailiff, *Radiat. Meas.* 27 (2) (1997) 185.
- [10] D. Mebhah, D. Imatoukene, F.Z. Abdelazziz, Z. Lounis-Mokrani, *Radiat. Meas.* 41 (7–8) (2006) 813.
- [11] W.F. Hornyak, R. Chen, A. Franklin, *Phys. Rev. B* 46 (13) (1992) 8036.
- [12] F.O. Ogundare, M.L. Chithambo, E.O. Oniya, *Radiat. Meas.* 41 (5) (2006) 549.
- [13] C.E. May, J.A. Partridge, *J. Chem. Phys.* 40 (1964) 1401.
- [14] Mahmoud Said Rasheedy, *J. Phys: Condens. Matter* 5 (1993) 633.
- [15] J. Garcia, V. Correcher, A. Delgado, L. Sanchez-Munoz, *Radiat. Meas.* 37 (2003) 473.
- [16] V. Correcher, J.M. Gomez-Ros, J. Garcia, A. Delgado, *Nucl. Instr. and Meth. A* 528 (2004) 717.
- [17] H.G. Balian, N.W. Eddy, *Nucl. Instr. and Meth.* 145 (1977) 389.
- [18] G. Guérin, A. Samper, *Radiat. Meas.* 42 (9) (2007) 1453.
- [19] Y.S. Horowitz, D. Satinger, D. Yossian, M.E. Brandan, A.E. Buenfil, L. Gamboa-deBuen, M. Rodriguez-Villafuerte, C.G. Ruiz, *Radiat. Prot. Dosim.* 84 (1999) 239.